A Study of Morphology and Intercalation Kinetics of Polystyrene−Organoclay Nanocomposites

ARTICLE *in* MACROMOLECULES · JUNE 2005

Impact Factor: 5.8 · DOI: 10.1021/ma0507084

2 AUTHORS, INCLUDING:

Hatsuo Ishida
Case Western Reserve University
448 PUBLICATIONS **12,888** CITATIONS

A Study of Morphology and Intercalation Kinetics of Polystyrene−Organoclay Nanocomposites

Yuqin Li and Hatsuo Ishida*

Department of Macromolecular Science and Engineering, Case Western Reserve University, Cleveland, Ohio 44106-7202

Received April 5, 2005; Revised Manuscript Received May 23, 2005

ABSTRACT: Temperature-modulated differential scanning calorimetry (TMDSC) is used to study the heat capacity (C_p) of monodisperse polystyrene in the nanocomposites. It is found that the bulk portion of polystyrene in the nanocomposites has a similar temperature range of glass transition behavior as pure polystyrene, while the normalized ΔC_p of polystyrene in the nanocomposites strongly depends on the polystyrene concentration. Results from TMDSC, especially the combination of kinetic study of TMDSC and X-ray diffraction, indicate that intercalated polystyrene does not contribute to the ΔC_p and does not have glass transition at the regular glass transition temperature. The maximum amount of intercalated polystyrene is around 40 wt %, and this amount will not increase as polystyrene concentration increases as long as the polystyrene with the same molecular weight is used. On the other hand, the amount of intercalated polystyrene increases when polystyrene molecular weight decreases.

Introduction

The interest in the field of polymer nanocomposites continues to be strong. Unlike typical composites, in which a reinforcing constituent is on the order of micrometers, nanocomposites utilize a constituent on the order of few nanometers, which is on the same scale as the radius of gyration of a polymer chain. The nanoscale distribution of the nanocomposites results in various advanced properties, including increased swelling resistance,[1] enhanced ionic conductivity,[2] and improved moduli.[3,4] Meanwhile, nanocomposites also provide the opportunity to explore new behaviors and morphologies of polymers. For example, it is known that there is significant overlap between polymer molecules in three dimensions, while in two dimensions, it has been suggested that different chains should overlap only slightly.[5] In the nanocomposites, polymer chains are restricted in the host silicate galleries of which spaces are smaller than or comparable to their dimensions. Their mobility and morphology should be dramatically different from their correspondent bulk not only due to the confinement of the polymer chains but also due to specific polymer−surface interactions. Research on this subject basically includes two major topics: crystallization behavior and glass transition behavior. Studies on different polymers, including poly(ethylene terephthalate) (PET),[6] poly(ethylene oxide) (PEO),[7] poly(ϵ-caprolactone),[8] and poly(vinylidene fluoride) (PVDF),[9] concluded that the mixing of polymer with clay would increase the nonisothermal crystallization rate of polymers and decrease the melting temperatures. The clay acting as a heterogeneous nucleating agent is considered to be the reason for rapid crystallization. However, many other studies based on the thermal analysis concluded that because of the confinement effect, polymer chains within the silicate layers cannot crystallize.[10,11] This indicates that the polymer conformation within the galleries may be different from that of the neat polymer, which has been confirmed by FTIR,[12] NMR,[13] and other techniques. For example, the OC−CO bond of poly(ethylene oxide) is found to be 90 ± 5% gauche within the silicate layers with the two-dimensional double-quantum NMR.[13]

On the other hand, there are various conclusions about the glass transition behavior of polymers within the silicate layers. While some papers claim that no change in the glass transition temperature is found for the polymer in the nanocomposites,[14] others reported an increase in the glass transition temperature, either slightly increase[15] or a huge increase that could not be detected.[16] Then, there are other reports about the decrease in the glass transition temperature for the nanocomposite system.[17] It is possible that the difficulty in the separation of the bulk portion from the intercalated portion is one of the major contributions to these contradictions for either the crystallization or the glass transition behavior.

To understand the structure and properties of surfactant and polymers in the nanoscopic space of the silicate galleries, it is necessary to look into more general nanoconfinement behavior. Confinement is achieved passively or actively depending on the existence of impenetrable surface such as solid substrate. In the case of the air−polymer interface, the polymer chains try to minimize the conformational energy by not going into the air. On the other hand, when a polymer chain is at an impenetrable solid wall, the polymer chains are forced to reflect from the substrate surface, as often the model adopted in Monte Carlo simulation. Nanoconfined structures commonly exist in our usual material investigation and applications. However, it is only very recently that interpretation of material structure and behavior has been attempted explicitly from nanoconfinement point of view, although there are many prior works that vaguely point to such directions. Earlier works that relate to confinement can be seen in the field of polymer adsorption. One of the earliest work in this area is the study of an isolated polymer chain at an interface by Frisch et al. using statistical mechanics.[18] A variety of theoretical treatments have been reported. The most prominent ones include the scaling theory by de Gennes,[19,20] the gradient term theory by Binder,[21,22] and the self-consistent-field theories with the lattice approach by Helfand[23,24] and Scheutjens and Fleer.[25,26] The concept of nanoconfinement started appearing in the literature about 10 years ago. The first

10.1021/ma0507084 CCC: $30.25
Published on Web 06/28/2005

comprehensive study for glass-forming material in highly confined geometries was the calorimetric study reported by Jackson and McKenna[27] and the first systematic study for very thin self-supported polymer films by Keddie et al.[28]

Confined polymer chains may attractively, neutrally, or repulsively interact with the substrate surface or air. Such variation complicates greatly the interpretation of the results, which lead to the confusing and sometimes conflicting results. This is one of the reasons why studies on free-standing films or surface with polymer/air interface have dominated the study of polymers under confinement, since the air/polymer interface is more quantifiable than the polymer/substrate interface. T_g of self-supported nanometer-thick films has been reported to be much lower than that of the bulk,[29] while the others reported no shift in T_g.[30,31] This was later found to be the complication caused by the polymer/substrate interaction. Using free-standing polystrene, reduction of T_g by 70 K for thickness of 29 nm has been reported.[32]

In a related subject of thin film T_g, an extensive investigation has been carried out on the surface T_g by the group of Kajiyama and Takahara in the past several years.[33−38] Conclusions common to these papers are that the T_g of the polymer surface is lower than the bulk, which is attributed to the segregation of the chain ends near the surface. Expectedly, this conclusion is the same as that obtained from free-standing thin films already described previously. They also reported that monodisperse polystyrene with molecular weight less than 30 000 is at the glass−rubber transition even at 293 K;[33,34] the T_g depression of polydisperse polystyrene is greater than the monodisperse samples due to the chemistry of the chain ends:[35] the surface has chain end segregation as determined by secondary ion mass spectroscopy depth profiling,[36] and polystyrene end-capped with a fluorinated group reduced T_g more than the proton end-capped polymer.[38] Thin, monodisperse polystyrenes terminated by proton and carboxylic acid group on a silane-treated silicon substrate show reduction of the degree of T_g suppression seen in the free-standing films by a strong film−substrate interaction.[37]

T_g depression of ultrathin films was explained by de Genne using the two competing motions: (i) standard motions which are controlled by the free volume and (ii) collective motions along the chain, which require a weaker free volume except for the end groups.[39] Many structural and conformational features of confined polymer chain behavior have been predicted by the Monte Carlo lattice and off-lattice computer simulations.[40−45] There is a paper claiming the inability to detect T_g for the materials under nanoconfinement.[36] All these are further complicated by a vast number of reports that T_g's of macroscopically filled polymers increase.[47] Also, nanocomposites increase,[48] exhibit no effect,[49] or decrease[50] T_g of the polymer matrix. Theory predicts decreased T_g of a confined polymer when the polymer interacts with the wall repulsively,[51] whereas the increased T_g is predicted under attractive interaction.[52] However, verification by experiment is far behind the theoretical work. This is in part due to the complicated nature of the polymer/substrate interaction and its difficulty in quantification. Clearly, carefully executed experimental verification, with familiarity with theoretical and other experimental confusion in the literature, must be carried out.

It is the purpose of this paper to probe the issue of glass transition behavior of polystyrene within the silicate galleries from the quantitative point of view based on the DSC thermal analysis and X-ray diffractometry. Additionally, the intercalation mechanism of polystyrene into the silicate galleries is of strong interest.

Experimental Section

Materials. Montmorillonite with a cation-exchange capacity (CEC) of 80 mequiv/100 g was supplied by Southern Clay Product. Hexadecylamine with purity of 98% was purchased from Aldrich Chemical Co. and was used as received. Polystyrene, with a weight-average molecular weight of 125 000−250 000, is purchased from Aldrich Chemical Co., and monodisperse polystyrenes with weight-average molecular weight and polydispersity index of 1.86×10^5, 1.07; 1.02×10^5, 1.02; 4.39×10^4, 1.01; 1.96×10^4, 1.01; 3.7×10^4; 1.03×10^4, 1.03; 5.4×10^3, 1.03; 2.8×10^3, 1.10; 946, 1.13; 550, 1.18; and 418, 1.13 were purchased from Toyo Soda Manufacturing Co., Tokyo, Japan.

Instruments and Methods. Organophilic montmorillonite was prepared by reacting original clay with hexadecylamine via both cation-exchange and ion−dipole intercalation methods. The cation-exchange method was done following ref 53. For the ion−dipole intercalation method, stoichiometric amounts of clay and hexadecylamine were mixed thoroughly with a spatula and annealed in a sealed vial at 120 °C for 40 min.

Polystyrene nanocomposites were prepared both from the solution method and the melt-blending method. For the solution intercalation, mixtures of polymer and solvent were stirred at elevated temperature for 1 h to obtain homogeneous solutions. Different amounts of cation-exchanged organoclay were added to the clear solutions, and the suspensions were stirred at 80 °C for 8 h. The dispersed clay systems were then cast into aluminum pans. The solvents were first evaporated at room temperature for 2 days and then dried in a vacuum oven, of which the temperature was gradually increased to 160 °C and was kept at this temperature for 10 h to ensure complete evaporation of the solvent. Melt intercalation was undertaken as follows. Particles of polymer and silicate with the required weight ratios of polymer-to-organoclay were roughly mixed using a spatula before being fed into a twin-screw extruder−microcompounder, Daca Instruments Inc. The mixing time was 10 min at 190 °C with a speed of 100 rpm.

For the kinetic study, desired amounts of clay powder and polymer powder were ground by a mortar and pestle and pressed into a pellet using a hydraulic press, Carver Laboratory Press, with a pressure of 4.45×10^7 Pa.

Wide-angle X-ray diffraction was performed by a Philips XRG 3100 diffractometer with Cu Kα radiation, using a scanning speed and step size of 0.06°/min and 0.01°, respectively. The data analysis is done with a commercial software (Grams 32) from Galactic Inc. Temperature-modulated differential scanning calorimetry (TMDSC) was performed using a 2920 MDSC from TA Instruments Inc. Temperature modulation was accomplished with a liquid nitrogen cooling accessory. Dry nitrogen gas with a flow rate of 80 mL/min was purged through the DSC cell. A heating rate of 2 °C/min with a temperature amplitude of ±2 °C and modulation period of 90 s was used. The temperature and heat flow were calibrated using water, indium, and zinc at 2 °C/min. Both the glass transition temperature and heat capacity (C_p) were obtained from the reversible heat flow curve. The glass transition temperature is marked as the temperature on the curve halfway between the two tangent lines, and C_p is obtained from the software, Universal Analysis, from TA Instruments.

Results and Discussion

Glass Transition. The formation of nanocomposites through both the solution intercalation and melt-blending methods is confirmed from the d spacing increment

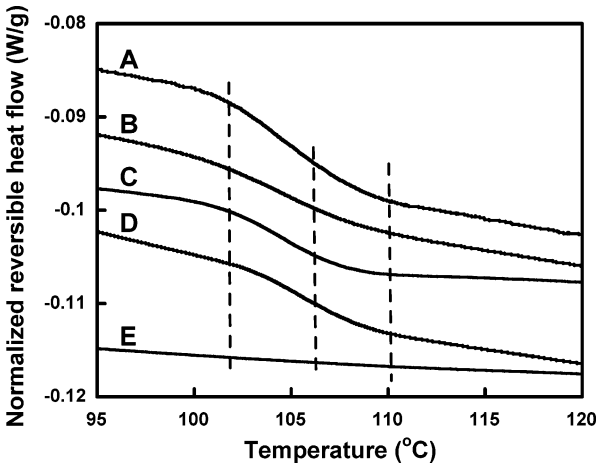

Figure 1. TMDSC thermograms of (A) pure PS, (B) PS microcompsite with 50 wt % of PS, (C) PS nanocomposites with 80 wt % of PS, (D) PS nanocomposite with 50 wt % of PS, and (E) PS nanocomposites with 17.6 wt % of PS. The weight-average molecular weight of polystyrene is 125 000−250 000.

by the X-ray diffraction method, which is described elsewhere.[54] The glass transition measurement is difficult for filled or reinforced polymer systems by ordinary DSC because the addition of filler would dilute the change of heat capacity at the glass transition temperature. By applying effectively two heating rates, the linear heating rate and sinusoidal heating rate, temperature-modulated DSC (TMDSC) separates irreversible heat flow from the reversible heat flow, increasing the sensitivity of the weak glass transition measurement. Therefore, the temperature-modulated DSC was used in the study of glass transition behavior of polystyrene nanocomposites to obtain more accurate and quantitative data. The TMDSC thermograms of pure polystyrene and polystyrene composites are illustrated in Figure 1. Both polystyrene microcomposite and nanocomposite have similar onset temperature, glass transition temperature, and end temperature as the pure polystyrene, which happens around 100−110 °C, except for some of the nanocomposite samples where the glass transition is not observed. Therefore, the apparent glass transition region is not broadened by the intercalation of polystyrene into the silicate layers due to the observation of the bulk polystyrene behavior only. No other glass transition behavior at high or low temperatures is observed in the temperature range of 20−200 °C studied. However, the normalized ΔC_p of polystyrene, which directly relates to the change of molecular mobility, strongly depends on the polymer concentration and distribution of the composites.

The normalized ΔC_p of polystyrene nanocomposites as a function of polystyrene concentration is shown in Figure 2, with the inserted figure as enlarged for low polystyrene concentration range. It should be reminded that the polystyrene concentration used is the weight ratio of polystyrene over clay. It is more straightforward to compare the amount of polymer with the amount of clay rather than the total amount of polymer and clay in order to quantitatively analyze intercalated polymer. The full range of Figure 2 shows the basic trend of ΔC_p: ΔC_p first increases quickly as polystyrene concentration increases and then levels off at the high concentration range. The asymptotic value is close to the value of pure polystyrene. The normalized ΔC_p of microcomposite with 50 wt % of polystyrene is similar to that of the pure polystyrene. This microcomposite was

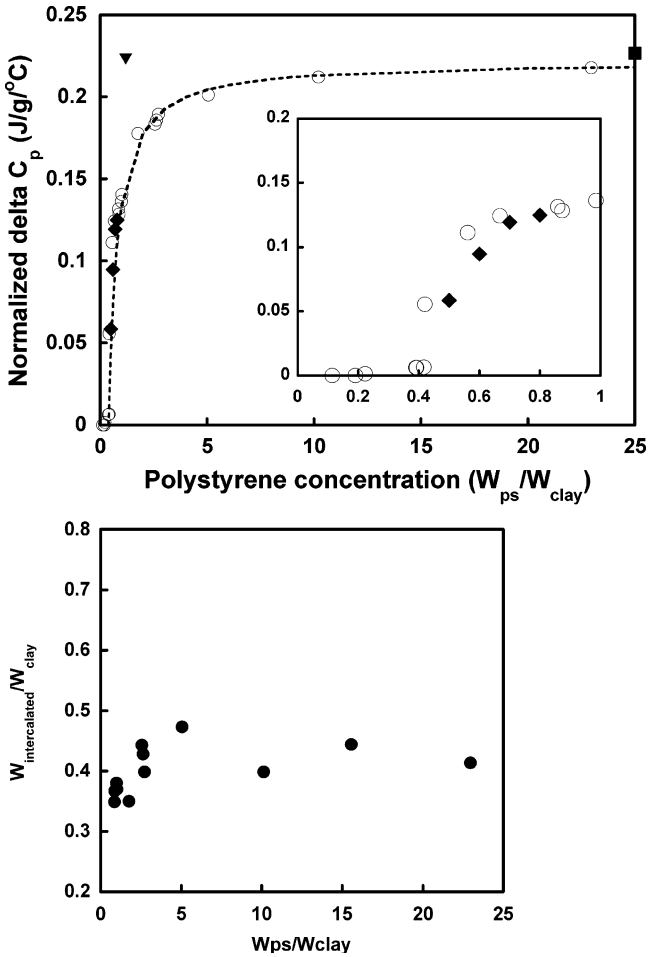

Figure 2. (top) Change of ΔC_p as a function of polystyrene concentration with inserted figure as the enlarged low concentration range. (○) PS nanocomposites prepared by the solution method, (◆) PS nanocomposites prepared by the melt method, (▼) PS microcomposite, and (■) pure PS. The weight-average molecular weight of polystyrene is 125 000−250 000. (bottom) The amount of intercalated polystyrene as a function of polystyrene concentration.

prepared from polystyrene and original inorganic clay instead of the amine-treated organoclay following the same preparation procedure as polystyrene nanocomposites. Because of the hydrophilic nature of the inorganic clay surface, polystyrene does not intercalate into the silicate layers; therefore, the dispersion is only in the microlevel. The same ΔC_p value of polystyrene in the microcomposite as that of the pure polystyrene means the microlevel dispersion would not change the ΔC_p of polystyrene.

The inset in Figure 2 shows a detailed concentration dependence of ΔC_p in the nanocomposites at the low polystyrene concentration range. Composites exhibit a ΔC_p value close to zero when polystyrene concentration is below 0.4. Because the sensitivity of TMDSC is sufficient to detect the ΔC_p of polystyrene in the microcomposite with the same polystyrene concentration, it is concluded that these nanocomposites with polystyrene concentration lower than 0.4 do not contribute to ΔC_p. Since the microdispersion would not change ΔC_p, the glass transition behavior of the polymer is influenced only when polystyrene intercalated into the silicate layers, indicating that the intercalated polystyrene does not have glass transition behavior at the regular glass transition temperature range. When polystyrene concentration increases to higher than 0.4,

ΔC_p increases drastically. Normalized ΔC_p can be calculated as

$$\Delta C_{p,\text{normalized}} = \frac{\Delta C_{p,\text{bulk}} W_{\text{bulk}} + \Delta C_{p,\text{intercalated}} W_{\text{intercalated}}}{W_{\text{PS}}} \quad (1)$$

where $\Delta C_{p,\text{normalized}}$, $\Delta C_{p,\text{bulk}}$, and $\Delta C_{p,\text{intercalated}}$ refer to the ΔC_p of normalized result of nanocomposites, bulk polystyrene, and intercalated polystyrene, respectively. W_{PS}, W_{bulk}, and $W_{\text{intercalated}}$ refer to the weight of the total polystyrene, bulk polystyrene, and intercalated polystyrene in the nanocomposites, respectively, and they follow that $W_{\text{PS}} = W_{\text{bulk}} + W_{\text{intercalated}}$.

When polystyrene concentration is larger than 0.4, with $\Delta C_{p,\text{intercalated}} = 0$, eq 1 can be rewritten as

$$\Delta C_{p,\text{normalized}} = \frac{\Delta C_{p,\text{bulk}}(W_{\text{PS}} - W_{\text{intercalated}})}{W_{\text{PS}}} \quad (2)$$

Therefore, the amount of intercalated polystyrene can be obtained from

$$\frac{W_{\text{intercalated}}}{W_{\text{clay}}} = \left(1 - \frac{\Delta C_{p,\text{normalized}}}{\Delta C_{p,\text{bulk}}}\right)\frac{W_{\text{PS}}}{W_{\text{clay}}} \quad (3)$$

In eq 3, $\Delta C_{p,\text{normalized}}$ is the experimental result from TMDSC, while W_{PS} and W_{clay} are obtained based on the results from TGA for the correspondent samples. The results calculated from eq 3 are shown in Figure 2. It can be seen that the change of overall polystyrene concentration does not cause much change in the intercalated polystyrene concentration. The value fluctuates between 0.35 and 0.45 no matter how the polystyrene concentration changes. This suggests that the intercalated polystyrene concentration is limited, and the further increase of polystyrene concentration would not promote the further intercalation, which agrees with the result that the d spacing would not change as polystyrene concentration increases.[16] A similar work stating the lack of cooperative motion in the bulk polymer starved layered silicate/poly(ethylene oxide) system was reported by Vaia et al.[46] Although the verification of complete intercalation and lack of the bulk polymer was not made, the trend obtained by the decreasing bulk polymer content supports the observation made in our study.

The conclusion that intercalated polystyrene would not contribute to the ΔC_p can be further confirmed by the kinetic study of the intercalation process. Figure 3 shows the X-ray diffraction curves of the organoclay and polystyrene mixture. Curve A, the room temperature mixture, shows the same diffraction pattern as the pure organoclay. Obviously, simply mixing the organoclay and polystyrene at room temperature would not change the structure, which corresponds to the result from the DSC shown in Figure 4 that the normalized ΔC_p of the mixture at the regular polystyrene glass transition temperature is the same as that of the pure polystyrene. After the mixture is annealed at 165 °C for 30 min, the d spacing of the clay is increased, which can be evidenced by the shift of diffraction peak to smaller diffraction angle shown as curve B in Figure 3, indicating the intercalation of polystyrene into the silicate layers. Meanwhile, curve B in Figure 4 for the 30 min annealed sample shows a clear decrease in the ΔC_p which can be seen from the decrease in the total area.

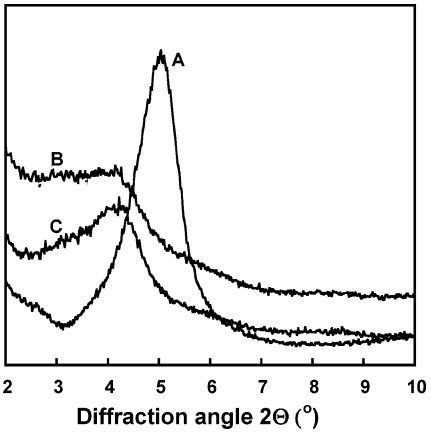

Figure 3. X-ray diffraction curves of (A) original mixture of organoclay and polystyrene, (B) the mixture after it was annealed at 165 °C for 30 min, and (C) the mixture after it was annealed at 165 °C for 60 min. The concentration of polystyrene in the mixture is 40 wt %.

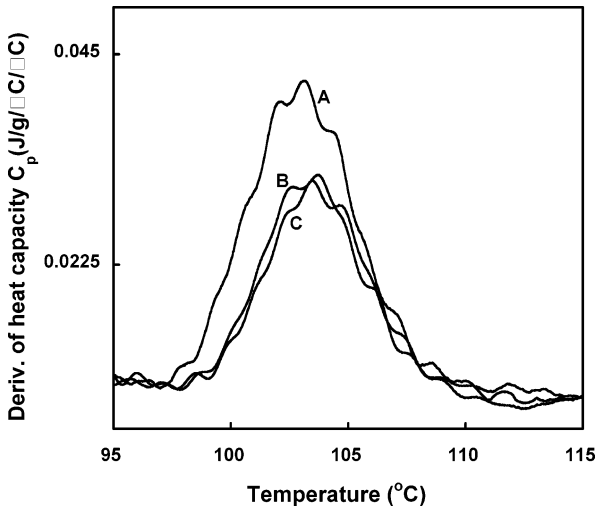

Figure 4. DSC curves of (A) original mixture of organoclay and polystyrene, (B) the mixture after it was annealed at 165 °C for 30 min, and (C) the mixture after it was annealed at 165 °C for 60 min. The concentration of polystyrene in the mixture is 40 wt %.

The further annealing did not result in any change in the d spacing in curve C in Figure 3, and it did not cause any change in the heat capacity change in curve C in Figure 4 either. Combining the result from X-ray diffraction in Figure 3 and the result from DSC measurement in Figure 4, we can conclude that the reduction in the ΔC_p is caused by the intercalation of polystyrene into the silicate layers.

Effect of Molecular Weight. The glass transition temperature of the bulk polystyrene depends on the molecular weight, as shown in Figure 5. These experimental results give a very nice fit to the Kanig–Ueberreiter equation[55]

$$\frac{1}{T_g(M_N)} = \frac{1}{T_g(\infty)} + \frac{K}{M_N}$$

with $K = 0.84$ and the asymptotic T_g value of 377 K. This expression is equivalent to the Fox equation[56] at high molecular weights but gives a better fit for PS of $M_N < 1$K. Compared to the pure polystyrene, the glass transition temperature of polystyrene nanocomposites shows a very close value when the molecular weight is

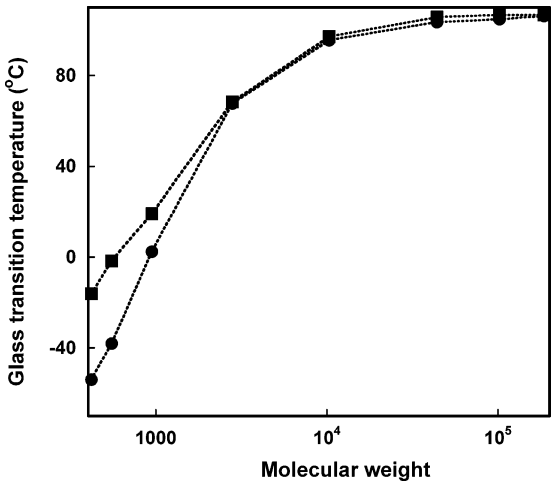

Figure 5. Influence of molecular weight on the glass transition temperature: (■) polystyrene nanocomposites and (●) pure polystyrene.

high; however, when the molecular weight is low, the glass transition temperature shows a drastic increase. Further study found that the glass transition temperature for the polystyrene microcomposites prepared from polystyrene and original inorganic clay shows a similar increase in the glass transition temperature when the polystyrene molecular weight is low. This means that the increase in the polystyrene glass transition temperature is not caused by the intercalation of polystyrene into the silicate layers; instead, it may be caused by the end group effect. As is well-known, the molecular weight dependence of glass transition temperature is caused by the end group effect. The end groups with large mobility occupy large composition for polymers with low molecular weight. Because of the interaction between the end group and clay surface, the mobility of end groups is decreased. Therefore, the end group effect on the glass transition temperature is weakened, resulting in higher glass transition temperature than the corresponding pure polystyrene sample. This may be one of the reasons why contradictory conclusions about glass transition temperature of materials under the confinement have often been reported. However, it is necessary to synthesize polystyrene with controlled end groups to further verify this hypothesis.

On the basis of the conclusion that intercalated polystyrene does not contribute to the ΔC_p, the intercalated amount of polystyrene can be calculated as a function of polystyrene molecular weight, which is shown in Figure 6. Since the final d spacing of polystyrene nanocomposites does not depend on the polystyrene molecular weight,[57] the increased amount of intercalated low molecular weight polymer might indicate the more available space that is not accessible to the larger molecules. However, more detailed, thermodynamically equilibrated systems need to be studied before understanding the origin of this phenomenon.

Intercalation Process. The intercalation process of polystyrene into the silicate galleries strongly depends on the polystyrene concentration. Basically, we can separate the concentration into roughly three regions based on the phenomenon observed during the intercalation process: low-concentration region that is below 50 wt %, medium-concentration region that is between 50 and 200 wt %, and high-concentration region that is above 200 wt %. It should be noted that these percentage values are relative to 100% clay. Shown in Figure

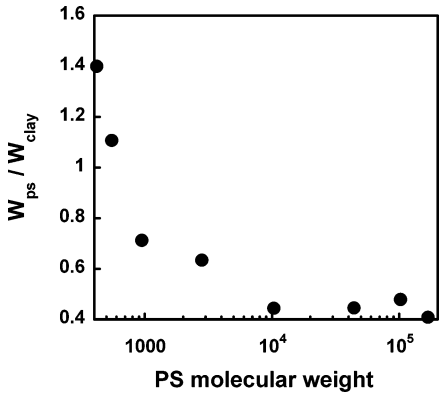

Figure 6. Intercalated amount of polystyrene as a function of polystyrene molecular weight.

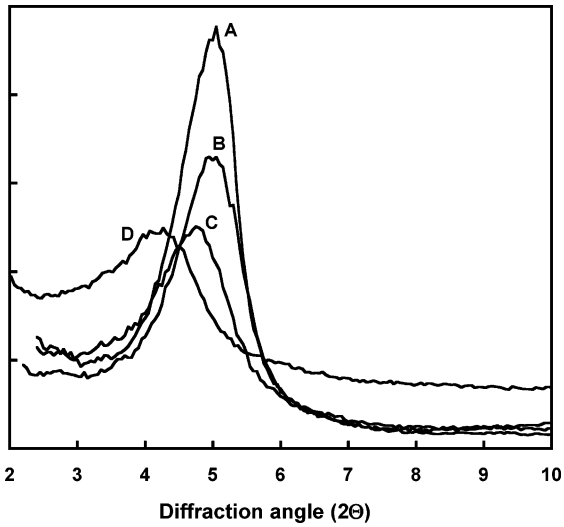

Figure 7. X-ray diffraction curves of polystyrene and organoclay mixture with polystyrene concentration at 30 wt %: (A) the original mixture, (B) after the mixture was annealed at 160 °C for 10 min, (C) after the mixture was annealed at 160 °C for 2 h, (D) after the mixture was regrind and annealed again at 160 °C for 30 min.

7 are the X-ray diffraction results for the mixture of polystyrene and clay with polystyrene concentration at 30 wt %. Annealing for the first 10 min did not cause much change in the diffraction angle; the intensity decreased drastically. During the following 2 h annealing, the diffraction angle shifted from the original diffraction angle of $2\theta = 5°$ ($d = 1.77$ nm) to small angles gradually. Further annealing beyond 2 h after that did not cause change in diffraction angle anymore. Then, the annealed sample was ground and repressed into a pellet. Grounding and pressing of the mixture at room temperature did not cause any change on the intercalation state of the sample. However, the diffraction angle gradually shifted to $2\theta = 4°$ ($d = 2.2$ nm) during the further annealing of the reground sample, and this is the final structure for the mixture with this range of concentrations.

For the mixture with polystyrene concentration between 60 and 200 wt %, the situation is quite different. The results for the mixture with 100 wt % of polystyrene are shown in Figure 8 as an example of this concentration range. The diffraction peak shifted from $2\theta = 5°$ to $2\theta = 4.4°$ during the first 10 min of annealing. Then, the diffraction angle gradually decreased to 4.2° and further to 4° during the following annealing. Additional annealing would not cause any further change. Again,

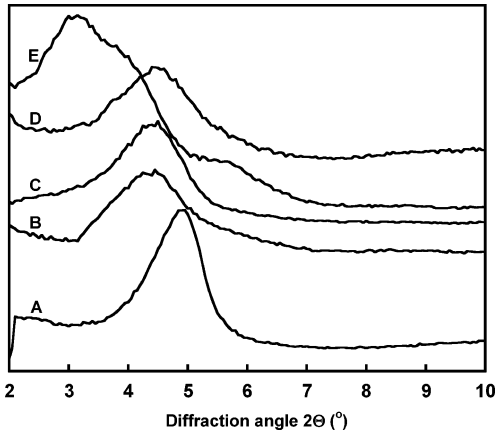

Figure 8. X-ray diffraction curves of polystyrene and organoclay mixture with polystyrene concentration at 10 wt %: (A) the original mixture, (B) after the mixture was annealed at 165 °C for 10 min, (C) after the mixture was annealed at 165 °C for 2 h, (D) after the mixture was regrind and repressed into pellet, (E) after the regrind sample was annealed at 165 °C for 10 min.

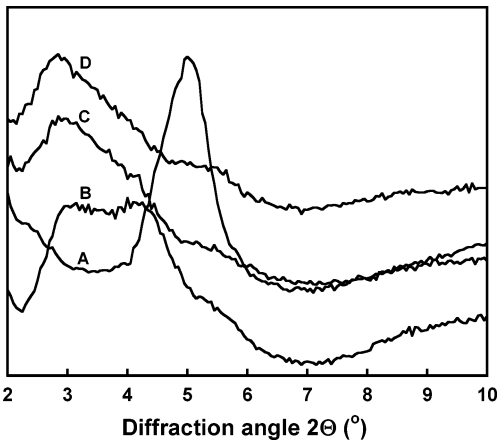

Figure 9. X-ray diffraction curves of polystyrene and organoclay mixture with 80 wt % polystyrene: (A) the original mixture, (B) after the mixture was annealed at 165 °C for 10 min, (C) after the mixture was annealed at 165 °C for 30 min, (D) after the reground and pressed pellet was annealed at 165 °C for 30 min.

after the reground sample was annealed for another 10 min, the diffraction angle shifted to $2\theta = 3°$ ($d = 2.94$ nm), and this would not change anymore during further annealing.

Figure 9 shows the X-ray diffraction results for the mixture with polystyrene concentration at 400 wt %. Two overlapped diffraction peaks at $2\theta = 3°$ and 4° are observed after the sample was annealed at 165 °C for 10 min. After further 10 min annealing, only the diffraction peak at $2\theta = 3°$ exists, while the diffraction peak at $2\theta = 4°$ disappeared. Nothing would change during the further annealing or regrinding, repressing, and annealing. Therefore, the completion of the intercalation process in this concentration range is a fast process.

It is obvious that the intercalation speed strongly depends on the polystyrene concentration; however, the first stage intercalation always happens quickly, although simply prolonging the annealing time would not reach the equilibrium intercalation state for the samples with relatively low polystyrene concentration. It is reasonable to assume that the intercalation of polystyrene into clay galleries relates to these different

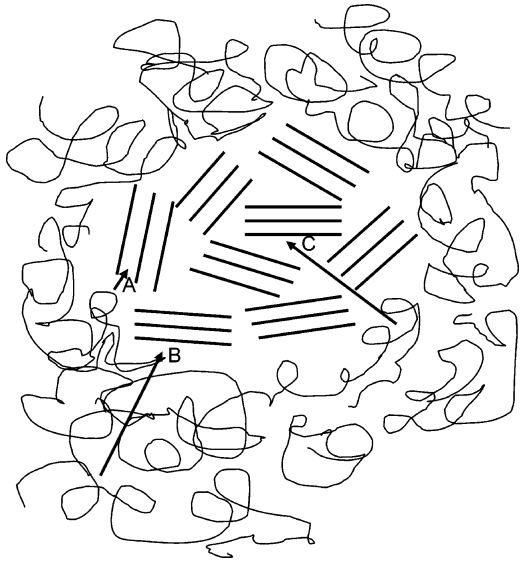

Figure 10. Schematic figure for the intercalation processes of polystyrene.

processes: (A) the intercalation of polystyrene from the clay edge, (B) resupply of polystyrene to the clay edge via diffusion, and (C) the distribution of polystyrene to the inside of clay particles, as schematically described in Figure 10. Since the first-stage intercalation happens within 10 min for all samples with different polystyrene concentrations, it is clear that the process (A), the intercalation of polystyrene from the clay edge, is a fast process. It is then the processes of (B) and (C) that control the further intercalation process. Consider the fact that the total amount of intercalated polystyrene is about 40 wt % based on clay, and this amount would not change as polystyrene solution concentration increases. This limited and constant amount of intercalation ability of polystyrene contributes to the process (C). In the low-concentration range, polystyrene is deficient in terms of the complete intercalation of clay; meanwhile, the low polystyrene concentration results in high viscosity, which makes it a slow process (B). Therefore, the complete intercalation can only be achieved after the regrinding and annealing to help redistribute the polystyrene. For the mixture with medium concentration of polystyrene, polystyrene concentration is sufficient for the complete intercalation of clay, but the rather low polystyrene concentration still needs regrinding and annealing for the complete intercalation. Only the mixture with high polystyrene concentration has low enough viscosity and oversaturated polymer concentration to finish the intercalation completely in minutes without regrinding.

Although the intercalation process strongly depends on the polystyrene concentration, there exist two common d spacings (diffraction angle): $d = 2.20$ nm ($2\theta = 4°$) and $d = 2.94$ nm ($2\theta = 3°$), which may be the thermodynamically stable states for the polystyrene intercalated nanocomposites. As we reported, one of the stable states of hexadecylamine intercalated clay has a d spacing of 2.94 nm ($2\theta = 3°$) where the orientation of amine chain is about 45° with the clay layers. We found that the d spacing of polystyrene nanocomposites is always 2.94 nm even when the organo-clay d spacing was changed from 5.04, 2.94, 2.20, to 1.77 nm by changing the degree of cation exchange. It was also reported by Vaia et al. that the final d spacing is the same for polystyrene with different molecular weight.[57]

It is possible that it is the amine orientation that controls the final d spacing of the polymer nanocomposites. While $2\theta = 3°$ is when the amine chains take the orientation about 45° with the clay layers, $2\theta = 4°$ is when the amine chains forms peso-trilayer for nonsufficient polystyrene intercalation.

Conclusion

Although contradictory results exist for the glass transition behavior of polymers within the silicate layers, the quantitative results from the temperature-modulated differential scanning calorimetry in this study clearly showed that intercalated polystyrene does not contribute to the ΔC_p, indicating that the intercalated polystyrene does not have glass transition behavior at the regular glass transition temperature. The contradiction may come from the fact that only a small amount of polymer can intercalate into the silicate layers. In the case of polystyrene and clay in this study, the total amount of intercalated polystyrene is almost constant at 40 wt % of clay weight no matter how much polystyrene concentration increases. The contradiction may also come from the fact that glass transition temperature of polystyrene would be largely influenced when the molecular weight is low, however, not by the intercalation but simply by mixing.

Acknowledgment. The authors gratefully acknowledge the financial support of the Federal Aviation Administration.

References and Notes

(1) Burnside, S. D.; Giannelis, E. P. *Chem. Mater.* **1995**, *7*, 1596.
(2) Wu, J.; Lerner, M. M. *Chem. Mater.* **1993**, *5*, 835.
(3) Messersmith, P. B.; Giannelis, E. P. *Chem. Mater.* **1994**, *6*, 1719.
(4) Yano, K.; Usuki, A.; Kurauchi, T.; Kamigaito, O. *J. Polym. Sci., Part A: Polym. Chem.* **1993**, *31*, 2493.
(5) De Gennes, P. G. *Scaling Concepts in Polymer Physics*; Cornell University Press: Ithaca, NY, 1979.
(6) Ke, Y.; Long, C.; Qi, Z. *J. Appl. Polym. Sci.* **1999**, *71*, 1139.
(7) Wang, Y.; Wu, B.; Yu, D. *Gaodeng Xuexiao Huaxue Xuebao* **1999**, *20*, 1143.
(8) Choi, H. K.; Park, Y. H.; Lyu, S. G.; Kim, B. S.; Sur, G. S. *Polymer* **1999**, *23*, 724.
(9) Priya, L.; Jog, J. P. *J. Polym. Sci., Part B: Polym. Phys.* **2002**, *40*, 1682.
(10) Messersmith, P. B.; Giannelis, E. P. *Chem. Mater.* **1993**, *5*, 1064.
(11) Vaia, R. A.; Vasudevan, S.; Krawiec, W.; Scanlon, L. G.; Giannelis, E. P. *Adv. Mater.* **1995**, *7*, 154.
(12) Aranda, P.; Ruiz-Hitzky, E. *Chem. Mater.* **1992**, *4*, 1395.
(13) Harris, D. J.; Bonagamba, T. J.; Schmidt-Rohr, K. *Macromolecules* **1999**, *32*, 6718.
(14) Tyan, H.-L.; Liu, Y.-C.; Wei, K.-H. *Chem. Mater.* **1999**, *11*, 1942.
(15) Agag, T.; Koga, T.; Takeichi, T. *Polymer* **2001**, *42*, 3399.
(16) Vaia, R. V.; Jandt, K. D.; Giannelis, E. P. *Chem. Mater.* **1996**, *8*, 2628.
(17) Chen, H. W.; Chiu, C. Y.; Chang, F. C. *J. Polym. Sci., Part B: Polym. Phys.* **2002**, *40*, 1342.
(18) Frish, H. L.; Simha, R.; Eirich, F. R. *J. Chem. Phys.* **1953**, *21*, 365.
(19) de Gennes, P. G. *Macromolecules* **1980**, *13*, 1069.
(20) de Gennens, P. G. *Macromolecules* **1981**, *14*, 1637.
(21) Binder, K. *J. Chem. Phys.* **1983**, *79*, 6387.
(22) Schmidt, M.; Binder, K. *J. Phys. (Paris)* **1985**, *46*, 1631.
(23) Helfand, E. *J. Chem. Phys.* **1975**, *63*, 2192.
(24) Helfand, E. *Macromolecules* **1976**, *9*, 307.
(25) Scheutjens, J. M. H. M.; Fleer, G. J. *J. Phys. Chem.* **1979**, *83*, 1619.
(26) Scheutjens, J. M. H. M.; Fleer, G. J. *J. Phys. Chem.* **1980**, *84*, 178.
(27) Jackson, L.; McKenna, G. B. *J. Non-Cryst. Solids* **1991**, *221*, 131.
(28) Keddie, J. L.; Jones, R. A. L.; Cory, R. A. *Europhys. Lett.* **1994**, *27*, 59.
(29) Reiter, G. *Europhys. Lett.* **1993**, *23*, 579.
(30) Keddie, J. L.; Cory, R. A. *Faraday Discuss.* **1994**, *98*, 219.
(31) Forrest, J. A.; Jones, R. A. L. In *Polymer Surfaces, Interfaces and Thin Films*; Karim, A., Kumar, S., Eds.; World Scientific: Singapore, 2000.
(32) Forrest, J. A.; Dalnoki-Veress, K.; Stevens, J. R.; Dutcher, J. R. *Phys. Rev. Lett.* **1996**, *77*, 2002.
(33) Tanaka, K.; Takahara, A.; Kajiyama, T. *Kobunshi Ronbunshu* **1996**, *53*, 582.
(34) Kajiyama, T.; Tanaka, K.; Takahara, A. *Bull. Chem. Soc. Jpn.* **1997**, *70*, 1491.
(35) Tanaka, K.; Takahara, A.; Kajiyama, T. *Macromolecules* **1997**, *30*, 6626.
(36) Kajiyama, T.; Tanaka, K.; Takahara, A. *Polymer* **1998**, *39*, 4665.
(37) Mounir, E. S. A.; Takahara, A.; Kajiyama, T. *Polym. J.* **1999**, *31*, 550.
(38) Jiang, X. Q.; Yang, C. Z.; Tanaka, K.; Takahara, A.; Kajiyama, T. *Phys. Lett. A* **2001**, *281*, 363.
(39) de Gennes, P. G. *Eur. Phys. J. E* **2001**, *2*, 201.
(40) Jiang, J. W.; Liu, H. L.; Hu, Y. *Macromol. Theory Simul.* **1998**, *7*, 105.
(41) Jiang, J. W.; Liu, H. L.; Hu, Y. *Macromol. Theory Simul.* **1998**, *7*, 113.
(42) Jang, J. H.; Mattice, W. L. *Polymer* **1999**, *40*, 4685.
(43) Jeon, J. H.; Kim, S. H.; Jo, W. H. *Macromol. Theory Simul.* **2002**, *11*, 147.
(44) Vacatello, M. *Macromol. Theory Simul.* **2001**, *10*, 187.
(45) Vao-soongnern, V.; Ozisik, R.; Mattice, W. L. *Macromol. Theory Simul.* **2001**, *10*, 553.
(46) Vaia, R. A.; Sauer, B. B.; Tse, O. K.; Giannelis, E. P. *J. Polym. Sci., Part B: Polym. Phys.* **1997**, *35*, 59.
(47) Ishida, H.; Koenig, J. L. *Polym. Eng. Sci.* **1978**, *18*, 128.
(48) Huang, J. C.; Zhu, Z. K.; Yin, J.; Qian, X. F.; Sun, Y. Y. *Polymer* **2001**, *42*, 873.
(49) Lopez, D,; Cendoya, I.; Torres, T.; Tejada, J.; Mijangos, C. *Polym. Eng. Sci.* **2001**, *41*, 1845.
(50) Liu, X. H.; Wu, A. J. *Polymer* **2001**, *42*, 10013.
(51) Haralampus, N.; Argiriadi, P.; Gilchriest, A.; Ashmore, E.; Scordalakes, C.; Martin, W.; Kranbuehl, D.; Verdier, P. *J. Noncryst. Solids* **1998**, *235*, 428.
(52) van Zenten, J. H.; Wallace, W. E.; Wu, W. L. *Phys. Rev. E* **1996**, *53*, R2053.
(53) Weiss, A.; Holm, C.; Platikanov, D. *Colloid Polym. Sci.* **1993**, *271*, 891.
(54) Li, Y. Q.; Ishida, H. *Polymer* **2003**, *44*, 6571.
(55) Ueberreiter, K.; Kanig, G. *J. Colloid Sci.* **1952**, *7*, 569.
(56) Fox, T. G.; Flory, P. J. *J. Appl. Phys.* **1950**, *21*, 581.
(57) Vaia, R. V.; Jandt, K. D.; Kramer, E. J.; Giannelis, E. P. *Chem. Mater.* **1996**, *8*, 2628.

MA0507084